Mitochondrial and Oxidative Stress Response in HepG2 Cells Following Acute and Prolonged Exposure to Antiretroviral Drugs

Savania Nagiah,[1] Alisa Phulukdaree,[2] and Anil Chuturgoon[1]*

[1]*Discipline of Medical Biochemistry, School of Laboratory Medicine and Medical Sciences, College of Health Sciences, University of KwaZulu Natal, Durban, South Africa*

[2]*Department of Physiology, Faculty of Health Science, University of Pretoria, Pretoria, South Africa*

ABSTRACT

Chronic HIV treatment with antiretroviral drugs has been associated with adverse health outcomes. Mitochondrial toxicity exhibited by nucleoside reverse transcriptase inhibitors (NRTIs) is pinpointed as a molecular mechanism of toxicity. This study evaluated the effect of NRTIs: Zidovudine (AZT, 7.1 μM), Stavudine (d4T, 4 μM) and Tenofovir (TFV, 1.2 μM), on mitochondrial (mt) stress response, mtDNA integrity and oxidative stress response in human hepatoma cells at 24 and 120 h. Markers for mt function, mt biogenesis, oxidative stress parameters, and antioxidant response were evaluated by spectrophotometry, luminometry, flow cytometry, qPCR and western blots. We found that AZT and d4T reduced mtDNA integrity (120 h, AZT: 76.1%; d4T:36.1%, $P < 0.05$) and remained unchanged with TFV. All three NRTIs, however, reduced ATP levels (AZT: 38%; d4T: 56.4%; TFV: 27.4%, $P = 0.01$) and mt membrane potential at 120 h ($P < 0.005$). Oxidative damage and reactive oxygen species (ROS) were increased by TFV and AZT at 24 h, and by d4T at 120 h ($P < 0.05$). Antioxidant response molecules and mt biogenesis markers were elevated by all NRTIs, with TFV causing the most significant increase ($P < 0.05$). Data from this study suggest that AZT, d4T and TFV alter mt function. TFV, however, achieves this independently of mtDNA depletion. Furthermore, AZT exerts toxicity soon after exposure as noted from changes at 24 h and d4T exerts greater toxicity over prolonged exposure (120 h). J. Cell. Biochem. 116: 1939–1946, 2015. © 2015 Wiley Periodicals, Inc.

Nucleoside reverse transcriptase inhibitors (NRTIs) form the backbone of combination antiretroviral therapy in HIV treatment. In developing countries, the massive rollout of these drugs favour standardised fixed dose combinations due to limited resources and cost effectiveness. Under these circumstances, the long term use of these drugs has seen the emergence of adverse health outcomes, particularly changes to metabolic parameters, lipodystrophy, dyslipidemia and hepatic steatosis [Carr and Cooper, 2000]. Investigation into antiretroviral therapy and their associated disorders found individual NRTIs had varying degrees of toxicity that are tissue specific and time dependent [Bleeker-Rovers et al., 2000; Birkus et al., 2002; Igoudjil et al., 2007; Kline et al., 2009].

Mitochondrial (mt) toxicity is a common outcome of NRTI use. Initially, thymidine analogues, including Zidovudine (AZT) and Stavudine (d4T), were considered to be the main culprits due to the inhibitory effect of these drugs on mtDNA replication [Brinkman et al., 1998]. However, other NRTIs, such as Tenofovir (TFV), still exhibit mt toxicity in spite of maintaining mtDNA levels [Kohler et al., 2009; Lebrecht et al., 2009]. This opened up investigations into alternate mechanisms of mt toxicity. Other proposed targets of NRTI toxicity include ATP synthesis, mt biogenesis, depleted native nucleotide pools, transcription of mtDNA, mt membrane integrity and transport and protein synthesis [Setzer et al., 2008; Cohen, 2010].

Oxidative stress and mt dysfunction are two closely linked outcomes of xenobiotic metabolism. Disruptions to mt function

increase the production of reactive oxygen species (ROS), especially superoxide ($O_2^{\bullet-}$), via defective oxidative phosphorylation. Elevated free radical production over a period of time depletes the antioxidant defence response, eventually resulting in oxidative damage to biomacromolecules including DNA, protein and lipid membranes.

The antioxidant defence system is regulated by the transcription factor, nuclear factor erythroid 2-related factor 2 (Nrf2). Nrf2 exists in the cytoplasm, bound to its inhibitor, Kelch-like associated ECH-associated protein (Keap1). In this state, Nrf2 is marked for degradation by ubiquitin, maintaining Nrf2 at low basal levels. Elevated ROS levels cause dissociation of Nrf2 from Keap1 by oxidizing the cysteine residues of the Nrf2–Keap1 complex. This allows Nrf2 to translocate to the nucleus and bind to the antioxidant response element (ARE), initiating the transcription of antioxidant (AO) genes such as superoxide dismutase (SOD), glutathione peroxidase (GPx), glutathione reductase and catalase [Motohashi and Yamamoto, 2004]. Aside from the endogenous antioxidant defence system, repair mechanisms are in place to compensate for oxidative damage. The high affinity for ROS to the guanine base in DNA results in DNA mutations and lesions. A base excision repair response to both nuclear and mtDNA damage is modulated by the enzyme, 8-oxoguanine DNA glycosylase (OGG1) [Stuart et al., 2004].

Mitochondria, being the main endogenous source of ROS, also require specialized defence mechanisms. An inner mitochondrial membrane protein, uncoupling protein2 (UCP2), is one such mechanism that functions to reduce ROS production by uncoupling oxidative phosphorylation from ATP synthesis. It achieves this by increasing proton conductance across the inner mt membrane, thus reducing ROS production during ATP synthesis [Nedergaard et al., 2005]. A common observation of mt toxicity is the up-regulation of mt biogenesis markers. The transcription of mt genes and mt biogenesis is regulated by a transcription co-activator, peroxisome proliferator-activated receptor γ co-activator 1α (PGC-1α). PGC-1α regulates mt gene transcription via interaction with nuclear respiratory factor 1 (NRF1) and 2, which in turn activates mt transcription factor A (TFAM) [Mallon et al., 2005]. Previous studies found that both PGC-1α and TFAM expressions were elevated in the presence of NRTIs, suggesting a nuclear response to mt toxicity [Mallon et al., 2005; Setzer et al., 2008]. Aside from its role in mt biogenesis, PGC-1α also acts as a modulator of mt AO response by increasing expression of oxidative stress protective genes [Valle et al., 2005; St-Pierre et al., 2006]. Mitochondrial AO responses such as PGC-1α and UCP2 are of importance as a known outcome of NRTI toxicity is oxidative stress [Lewis et al., 2001; Manda et al., 2011].

Naturally, the nature of NRTI toxicity results in mitochondria-rich tissues being the most affected following chronic exposure [Dagan et al., 2002]. The liver being the metabolic hub of humans is abundant in mitochondria. The HepG2 cell line has been widely used in previous studies evaluating the effect of antiretroviral drugs on mitochondrial toxicity [Birkus et al., 2002; Walker et al., 2002; Velsor et al., 2004; de Baar et al., 2007; Setzer et al., 2008]. HepG2 cells possess cytochrome P_{450} activity and has hence been identified as an early model for xenobiotic metabolism [Roe et al., 1993]. Nucleoside reverse transcriptase inhibitors, including AZT and Stavudine, require intracellular phosphorylation to their triphosphate active form. It is only in this form that the drugs may incorporate into DNA, exerting an effect. The cytochrome P_{450} activity of HepG2 cells is integral to the biotransformation of NRTIs. This study aimed to investigate the effects of three commonly used NRTIs: AZT, d4T and TFV on mt function and AO response; focussing on Nrf2 and PGC-1α mediated stress responses, in HepG2 liver cells following exposure for 24 and 120 h.

MATERIALS AND METHODS

MATERIALS
All reagents were purchased from Merck (Darmstadt, Germany), unless otherwise stated. Cell culture media were obtained from Lonza, Biowhittaker (Johannesburg, South Africa), and supplements were purchased from Sigma–Aldrich (St. Louis, MO). All antiretroviral drugs were obtained from the NIH Aids reagents programme. Antibodies utilized for western blots were purchased from Cell Signalling Technology, Inc (Beverly, MA).

CELL CULTURE AND TREATMENT
Human hepatoma (HepG2) cells were cultured in supplemented Eagle's minimum essential media (10% foetal calf serum, 1% penstrepfungizone, 1% L-glutamine) at 37°C in a humidified incubator. Cells were seeded in sterile 25 cm^3 cell culture flasks and subjected to treatment once the cells were 80% confluent.

Stocks of NRTIs (10 mM in dimethylsulphoxide) were prepared. HepG2 cells were treated with NRTIs at maximum plasma level concentrations [Walker et al., 2002; Venhoff et al., 2007]. Treatments with AZT (7.1 μM), d4T (4 μM), TFV (1.2 μM) and an untreated control were conducted over two time periods (24 and 120 h). For the 120 h treatment, fresh cell culture medium containing NRTI treatment was replenished every 48 h.

LIPID PEROXIDATION
Lipid peroxidation was used as a marker of oxidative stress. The thiobarbituric reactive substances (TBARS) assay was used to quantify extracellular malondialdehyde (MDA), a by-product of lipid peroxidation. Following treatments, 2 ml of supernatant from each treatment was aspirated and freeze dried. The lyophilised supernatants were then reconstituted in 500 μl of 0.1 M phosphate saline buffer (PBS) and used for the TBARS assay. The TBARS assay was conducted as per the method described by Phulukdaree et al. [2010]. Absorbance of the samples was read using a spectrophotometer, $\lambda = 532/600$ nm (Bio-Tek μQuant, Winooski, VT). MDA concentrations (mM) were calculated by dividing the mean absorbance of the samples by the absorption coefficient (156 mM^{-1}).

INTRACELLULAR REACTIVE OXYGEN SPECIES
Intracellular ROS (Superoxide: $O_2^{\bullet-}$, hydrogen peroxide, peroxynitrite) was quantified by fluorescence activated cell sorting (FACS) using the fluorescent probe, 2′,7′-dichlorodihydrofluorescein diacetate (H2DCF-DA). Following exposure to NRTIs (24 and 120 h), 1×10^6 HepG2 cells were incubated in phenol red-free media supplemented with 10% foetal calf serum and 10 μM H2DCFA for 45 min at 37°C. The probe diffuses into the cell and is retained intracellularly, until it is cleaved by intracellular esterases to the

non-fluorescent 2′,7′-dichlorodihydrofluorescein (H2DCF). Intracellular ROS oxidise H2DCF to 2′,7′-dichlorofluorescein (DCF) which emits fluorescence at 525 nm. Stained cells were rinsed thrice with 0.1 M PBS (400g, 5 min, RT) and resuspended in 150 µl of 0.1 M PBS. Fluorescence of 20,000 events was measured using the FL-1 channel (525 nm) of the Accuri^{TM} C6 flow cytometer (BD Biosciences, Franklin Lakes, NJ). Live cells were gated using CFlow Plus Software (BD Biosciences, San Jose, CA). Results were reported as percentage DCF positive.

JC-1 MITOSCREEN

The percentage mitochondrial depolarisation ($\Delta \psi_m$) was measured using FACS and the JC-1 Mitoscreen (BD Biosciences, San Jose, CA). Briefly, JC-1 stock solution was diluted in 1X Assay Buffer (37°C) to make up a working solution. Approximately 200,000 cells suspended in 100 µl of 0.1 M PBS from each treatment were transferred to 1.5 ml tubes containing 100 µl of JC-1 staining solution and incubated (10 min, 37°C). Thereafter, 100 µl of FACS sheath fluid was added to each sample. Flow cytometry data from stained cells (50,000 events) were captured with the Accuri^{TM} C6 flow cytometer and software (BD Biosciences). Live cells were gated using CFlow Plus Software (BD Biosciences).

REDUCED AND TOTAL GLUTATHIONE

The endogenous antioxidant, reduced glutathione (GSH) was measured by the GSH-Glo^{TM} Glutathione Assay (Promega, Madison, WI) as per the manufacturer's instructions. Both reduced glutathione (GSH) and a total of reduced and oxidized glutathione (GSSG) were quantified. The total amount of glutathione present (GSH + GSSG) was quantified by addition of Tris-(2-carboxyethyl)-phosphine (TCEP) which reduces GSSG to GSH.

Briefly, six GSH standards were prepared (0–50 µM) to derive a standard curve. Fifty microlitres of cell suspension (20,000 cells)/standard solution was aliquot in a white microtitre plate. For the quantification of GSH + GSSG, 10 µM of TCEP was added per well. Thereafter, 50 µl GSH-Glo^{TM} Reagent (1 µl Luciferin-NT, 1 µl Glutathione-S-transferase, 48 µl GSH-Glo^{TM} Reaction buffer) was added per well and incubated for 30 min. Luminescence was measured on a Modulus^{TM} microplate luminometer (Turner BioSystems, Sunnyvale, CA).

ATP

ATP was measured by the luminometric Cell Titer-Glo® assay. Cells were aliquoted in a white microtitre plate (20,000 cells per well) in a 1:2 ratio with ATP Cell Titer-Glo® Reagent (Promega). The plate was incubated for 30 min at RT. Luminescence was measured on a Modulus^{TM} microplate luminometer (Turner BioSystems). Luminescence is proportional to ATP concentration and was expressed as relative light units (RLU).

RNA ISOLATION AND QUANTITATIVE PCR

Complementary DNA (cDNA) was synthesized from RNA for quantitative PCR (qPCR). Total RNA was isolated using an in-house protocol [Chuturgoon et al., 2014]. RNA concentrations were determined (Nanodrop 2000, ThermoScientific, South Africa) and standardised to a concentration of 1,000 ng/µl. RNA was then converted to cDNA using the iScript^{TM} cDNA Synthesis kit (BioRad;

catalog no. 107-8890). A reaction volume of 20 µl containing 4 µl of 5X iScript reaction mix, 1 µl of iScript reverse transcriptase and 2,000 ng of RNA template were made up in nuclease free water. Thermocycler conditions for cDNA synthesis were 25°C for 5 min, 42°C for 30 min, 85°C for 5 min and a final hold at 4°C.

Gene expression of oxidative DNA damage response (*OGG1*) and mitochondrial transcription (*TFAM*) were determined by qPCR. The iQ^{TM} SYBR® Green Supermix (BioRad, 170–880) was used to measure mRNA levels of the genes of interest. Briefly, 1.5 µl of cDNA template was added to 1 µM of sense primer (*TFAM*: 5′-TATCAAGTGCTTATAGGC-3′; *OGG1*: 5′-GCATCGTACTCTAGCCTC-CAC-3′), 1 µM antisense primer (*TFAM*: 5′-CACTCCTCAGCACCA-TATTTCG-3′; *OGG1*: 5′-AGGACTTTGCTCCCTCCAC-3′), 5X iScript reaction mix and nuclease free water in a final reaction volume of 25 µl. Initial denaturation was conducted at 95°C for 4 min, followed by 37 cycles of denaturation (95°C; 15 sec), annealing [50°C (*TFAM*)/60°C (*OGG1*); 40 sec], and extension (72°C; 30 sec).

All qPCR experiments were conducted on the CFX96 Touch^{TM} Real-Time PCR Detection System (BioRad, Hercules, CA). Changes to gene expression were calculated according to the methods described by Livak and Schmittgen [2001]. Results are converted from mean relative fold change ($2^{-\Delta\Delta Ct}$) to percentage mRNA expression relative to the untreated control (100%). A minimum of three housekeeping genes, β-actin (sense: 5′-TGACGGGTCACCCACACTGTGCCCAT-3′; antisense: 5′-CTAGAAGCATTTGCGGTGGACGATGGAGGG-3′); GAPDH: (sense: 5′-TCCACCACCCTGTTGCTGTA-3′; antisense: 5′-ACCACAGTCCATGCCATCAC-3′); 18S: (sense: 5′-ACAGGGACAG-GATTGACAGA-3′; antisense: 5′-CAAATCGCTCCACCAACCTAA-3′) was amplified simultaneously under the same conditions.

MITOCHONDRIAL DNA VIABILITY

DNA was isolated from cell suspensions as described by Sambrook [2001]. Isolated DNA was quantified using the Nanodrop 2000 spectrophotometer and standardised to 5 ng/µl. A reaction volume of 25 µl consisting of 12.5 µl SYBR Green Supermix (BioRad), 10 $p$mol of forward (5′-TGAGGCCAAATATCATTCTGAGGGC-3′) and reverse primer (5′-TGCACCTGCTCTCTGTGATTATGACTATCCCACAGTC-3′), and ~10 ng DNA template made up in nuclease free water. Changes in mtDNA application were calculated based on the method described by Livak and Schmittgen [2001] and reported as percentage mtDNA amplification relative to untreated control (100%). A house keeping gene, β-globin (sense: 5′-ACATGATTAGCAAAGGGCCTAGCTTGACT-CAGA-3′; antisense: 5′-TGCACCTGCTCTCTGTGATTATGATATCC-CACAGTC-3′) was amplified simultaneously. Initial denaturation was applied (94°C; 3 min), followed by 28 cycles of denaturation (94°C; 20 sec); annealing (58°C; 10 min), extension (72°C; 10 min) and a plate read. This was followed by a melt curve and a final hold (25°C; 5 min).

WESTERN BLOTS

Protein expression of PGC-1α, Nrf2, UCP2 and SOD1 were determined using western blots. Briefly, 200 µl of Cytobuster (Novagen, San Diego, CA) supplemented with protease and phosphotase inhibitors (Roche, Mannheim, Germany) was added to treated cells in cell culture flasks and kept on ice for 30 min before being scraped and transferred to 1.5 ml tubes. The cell lysates were centrifuged (13,000g, 10 min). Crude protein was quantified using

the bicinchoninic assay. All protein samples were standardised to 2 mg/ml. Laemmeli buffer [dH$_2$O, 0.5 M Tris-HCl (pH 6.8), glycerol, 10% SDS, β-mercaptoethanol, 1% bromophenol blue] was added to the samples (1:1 ratio) and boiled for 5 min. Samples were separated by electrophoresis on a SDS polyacrylamide gel (4% stacking and 10% resolving) for 1 h at 150 V. The separated proteins were transferred to a nitrocellulose membrane using the TransBlot Turbo Transfer System (BioRad) at 400 mA for 45 min. Membranes were incubated in a blocking solution of 5% bovine serum albumin (BSA) in Tween 20-Tris buffered saline (TTBS) for 1 h at RT. The membranes were incubated with primary antibody [mouse anti-SOD1 (CS4266), rabbit anti-Nrf2 (ab31163), goat anti-UCP2 (ab77363), rabbit anti-PGC-1α (CS2178), 1: 1,000 dilution in 1% BSA] for 1 h at RT, and then overnight at 4°C. The membranes were washed five times with TTBS (10 min) before being incubated in HRP-conjugated secondary antibody [goat anti-mouse (31800); goat anti-rabbit (ab6112) 1:10 000 in 1% BSA] for 1 h at RT. The membranes were then washed five times in TTBS (10 min). Clarity Western ECL Substrate (BioRad) detection reagent was used to visualise protein bands. Images were captured using gel documentation system Alliance 2.7 (UViTech). Relative band density (RBI) was measured by densitometric analysis using UViTech Alliance Analysis software.

Membranes were stripped with 5% hydrogen peroxide, incubated in blocking solution (3% BSA; 1 h; RT), rinsed twice in TTBS and probed with HRP-conjugated antibody for the house-keeping protein, β-actin (Sigma, St Louis, MO). The relative band intensity was normalised against β-actin and then reported as fold change relative to the control.

STATISTICAL ANALYSIS

Statistical analyses were performed using the GraphPad Prism V5 software package (GraphPad Software, Inc., San Diego, CA). All data sets were assessed for Gaussian distributions using the D'Agostino & Pearson omnibus normality test. Comparisons between the control and drug treatments were done by performing Kruskal–Wallis tests (nonparametric distributions).

RESULTS

OXIDATIVE DAMAGE AND INTRACELLULAR ANTIOXIDANT LEVELS

HepG2 cells exposed to AZT and TFV for 24 h had higher levels of intracellular ROS (Fig. 1A; $P = 0.02$) and MDA levels ($P = 0.02$; Fig. 1B) relative to the untreated control. In the same time period, no
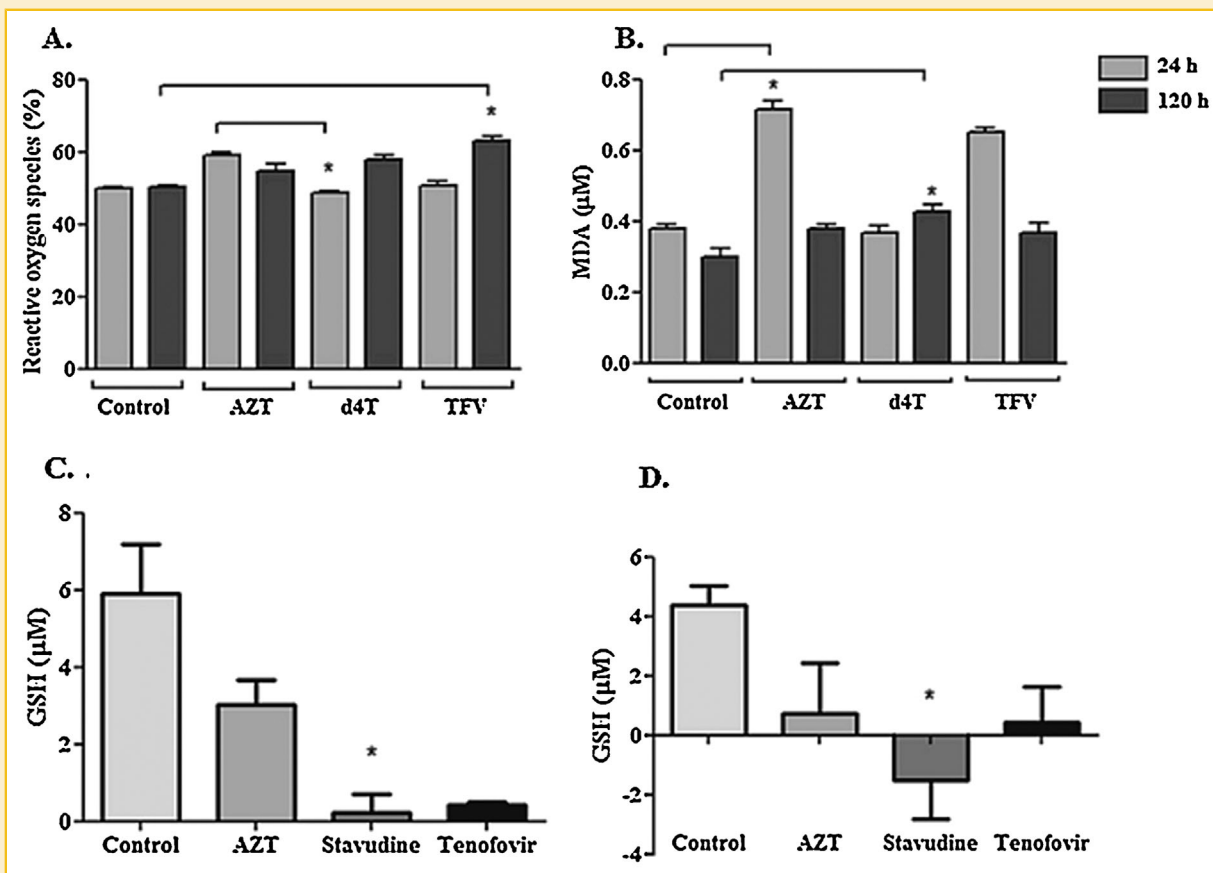

Fig. 1. Intracellular reactive oxygen species measured as DCF fluorescence (A), extracellular malondialdehyde levels (B), GSH (C) and total glutathione (GSH + GSSG; D) in HepG2 cells treated with NRTIs at 24 and 120 h, *$P < 0.05$ relative to control.

TABLE I. Percentage Regulation Analysis of mRNA Expression (*OGG1*; *TFAM*) and mtDNA Amplification Relative to Untreated Control at 24 and 120 h Treatment With NRTIs

	Viable mtDNA	*TFAM*	*OGG1*
24 h			
AZT	184 (168, 211)	105 (51.1, 169)	44.5 (36.5, 60.3)*
d4T	69.56 (53.6, 84.9)	6.37 (4.51, 9.19)**	2.98 (1.68, 3.69)***
TFV	151 (95.2, 251)	98.1 (82.8, 106)	56.7 (53.9, 58.23)
120 h			
AZT	76.1 (65.3, 83.3)*	830 (748, 942)***	104 (982, 117)
d4T	36.1 (15.0, 76.4)*	278 (264, 304)	98.1 (82.8, 106)**
TFV	189.4 (144, 214.6)	633 (557, 740)*	1047 (980, 1170)***

AZT, zidovudine; d4t, stavudine; TFV, tenofovir; mt, mitochondrial; TFAM, mitochondrial transcription factor A; OGG1, 8-oxoguanine DNA glycosylase.
Data represented as median (IQR) *$P < 0.05$; **$P < 0.005$; ***$P < 0.0001$ relative to control (100%).

significant changes were observed in the intracellular ROS and MDA levels of cells exposed to d4T ($P > 0.05$). Following 120 h exposure, all three drugs increased both intracellular ROS (Fig. 1A) and extracellular MDA levels (Fig. 1B) compared to the control. Intracellular ROS levels were significantly higher in the TFV treated cells at 120 h ($P = 0.02$), and d4T caused the greatest increase in MDA levels ($P = 0.02$).

At 24 h, base excision repair response, *OGG1*, was down-regulated in all treatments, most so in the AZT and d4T treatment ($P < 0.0001$; Table I). However, after 120 h, all three NRTIs increased *OGG1* mRNA levels relative to the control (Table I). Most notably, there was a 10-fold increase in the d4T and TFV treatments ($P = 0.0003$).

After 24 h exposure, AZT increased both GSH ($P = 0.04$, Fig. 1C) and GSH + GSSG ($P = 0.02$, Fig. 1D) levels relative to the control. In the same time period, d4T reduced both GSH (Fig. 1C) and GSH + GSSG (Fig. 1D). HepG2 cells exposed to TFV for 24 h showed lowered GSH levels (Fig. 1C) but GSH+GSSG levels remained similar to the control (Fig. 1D). After 120 h, there was no statistical significant change in GSH levels in NRTI treated HepG2 cells as compared to the untreated cells ($P = 0.06$; Fig. 1B). Total glutathione (GSH + GSSG) was only increased by TFV at 120 h ($P = 0.02$; Fig.

1D), whilst AZT and d4T decreased GSH + GSSG relative to the control.

MITOCHONDRIAL INTEGRITY AND FUNCTION

Mitochondrial membrane depolarisation and ATP were measured as mt function parameters. At both time periods, AZT and TFV markedly reduced ATP levels (24 h: $P = 0.0.1$; 120 h: $P = 0.02$, Fig. 2A) with a concomitant increase in $\Delta\psi_m$ (24 h: $P = 0.12$; Fig. 2B; 120 h: $P = 0.02$; Fig. 2B). ATP levels remained unchanged at 24 h in the d4T treatment, but a marked decline was observed at 120 h (Table I). Percentage $\Delta\psi_m$ was elevated in HepG2 cells exposed to d4T for 24 h, but not significantly ($P = 0.02$; Fig. 2B).

The mt response to $O_2^{\bullet-}$ production was evaluated by quantifying UCP2 expression. At 24 h, UCP2 protein expression increased in the AZT [1.75 RBI (Inter-quartile range: IQR: 1.70, 1.81)] and d4T treatment [1.80 RBI (IQR: 1.60, 2.18)] relative to the control [1.49 RBI (IQR: 1.26, 1.74); Fig. 3]. The 120 h treatment showed an increase in UCP2 expression in the NRTI treated cells [Control: 1.37 RBI (IQR: 1.20, 1.58); AZT: 1.53 RBI (IQR: 1.42, 1.68); d4T: 1.74 RBI (IQR: 1.63, 1.93)], with a significant increase in the TFV treatment [2.02 RBI (IQR: 1.87, 2.15); $P = 0.04$; Fig. 3].
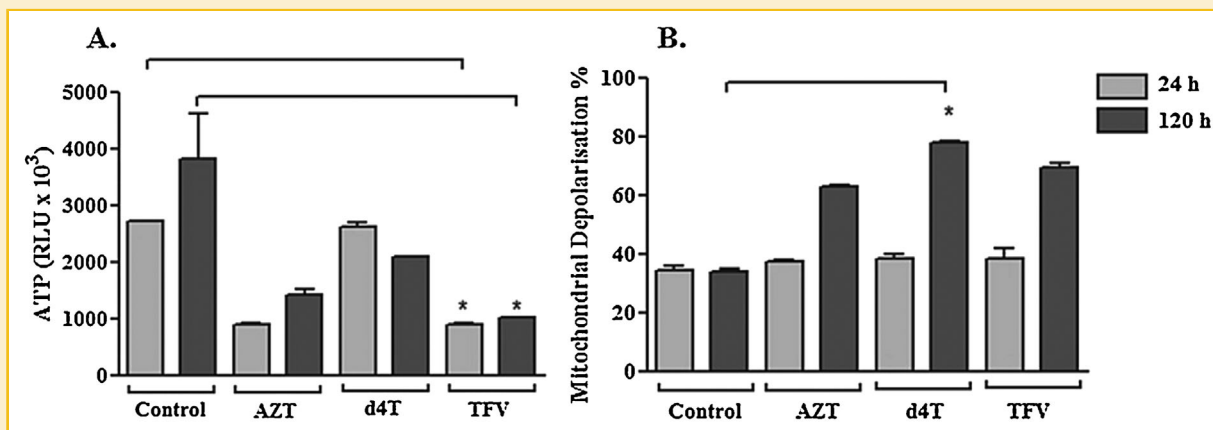

Fig. 2. ATP levels (A) and mitochondrial (mt) depolarisation (B) in HepG2 cells treated with zidovudine (AZT), stavudine (d4t) and tenofovir (TFV) at 24 and 120 h, *$P < 0.05$ compared to untreated control. RLU, relative light units.
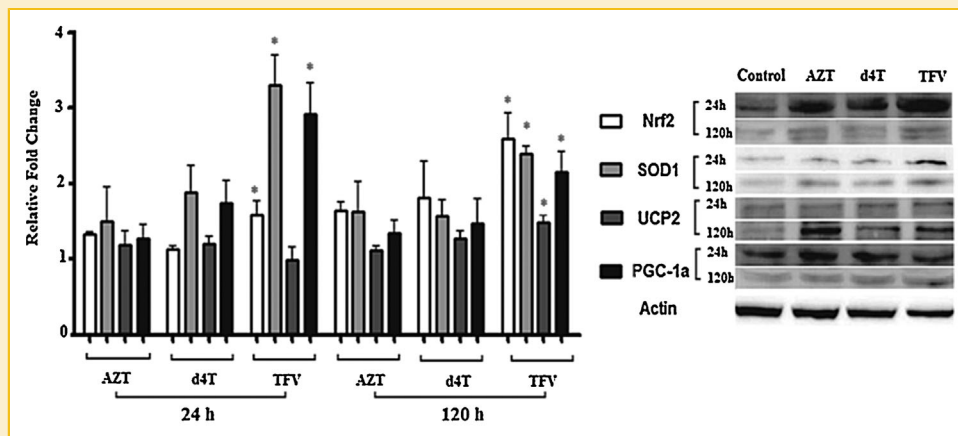
Fig. 3. Densitometry analysis and western blot images for antioxidant and mitochondrial oxidative stress response protein expression at 24 and 120 h treatment with NRTIs. *P < 0.05 relative to control.

Protein expression of PGC-1α, a regulator of mt biogenesis, was assessed as a response to mt damage, while *TFAM* mRNA levels evaluated mtDNA transcription. The qPCR results showed that *TFAM* mRNA levels at 24 h was not differentially regulated in the TFV and AZT treatments (Table I). Stavudine, however, significantly reduced *TFAM* mRNA levels at 24 h ($P = 0.003$; Table I). Following 120 h exposure, *TFAM* mRNA levels increased in all NRTI treated HepG2 cells exceeding twofold ($P < 0.0001$; Table I). Expression of PGC-1α protein was also elevated by all three NRTIs at both 24 h [AZT: 3.24 RBI (IQR: 3.16, 3.33); d4T: 4.44 RBI (IQR: 4.21, 4.76)] and 120 h [AZT: 2.7 1RBI (IQR: 2.51, 2.91); d4T: 2.94 RBI (IQR: 2.30, 3.40)] compared to their respective controls [Control 24 h: 2.57 RBI (IQR: 2.19, 2.96); Control 120 h: 2.01 RBI (IQR: 1.89, 2.10)]. Tenofovir induced significantly higher expression of PGC-1α in both time periods [24 h: 7.38 RBI (IQR: 6.69, 8.11); $P = 0.02$; 120 h: 4.32 RBI (IQR: 4.0, 4.63); $P = 0.02$; Fig. 3].

The amount of viable mtDNA in each treatment was determined by qPCR. This assay works on the principle that viable mtDNA levels will be proportional to mtDNA amplification. The AZT and TFV treatments caused an increase in mtDNA amplification relative to the control following 24 h exposure (Table I). The d4T treatment, however, decreased the amount of viable mtDNA in this time period ($P = 0.04$; Table I). At 120 h, AZT also caused a decline in mtDNA integrity and a significant decrease was observed in the d4T treatment ($P = 0.01$). Tenofovir still exhibited increased mtDNA amplification at 120 h (Table I).

ANTIOXIDANT RESPONSE

The expression of key AO proteins was measured to determine the AO response induced by NRTIs. At 24 h, only TFV significantly increased Nrf2 protein expression in HepG2 cells [8.40 RBI (IQR: 7.05, 9.28); $P = 0.01$; Fig. 3] compared to the control [5.26 RBI (IQR: 5.02, 5.50); Fig. 3]. At 120 h, however, the expression of Nrf2 was elevated by d4T [5.04 RBI (IQR: 4.63, 5.82)] and AZT treatments [4.68 RBI (IQR: 3.86, 5.36)] relative to the control [2.83 RBI (IQR: 2.49, 3.30)], and

significantly up-regulated by TFV [7.22 RBI (IQR: 6.83, 7.88); $P = 0.02$; Fig. 3].

SOD1 regulates both mitochondrial and cytosolic detoxification of $O_2^{\bullet-}$. Only TFV significantly up-regulated protein expression of SOD1 at 24 h [0.34 RBI (IQR: 0.33, 0.35); Fig. 3] and 120 h [6.35 RBI (IQR: 6.15, 6.72); $P = 0.02$; Fig. 3] compared to the control (Fig. 3). Stavudine [24 h: 0.02 RBI (IQR: 0.02, 0.02); 120 h: 4.18 RBI (IQR: 3.54, 4.50)] and AZT [24 h: 0.02 RBI (IQR: 0.01, 0.02); 120 h: 4.33 RBI (IQR: 3.36, 5.51)] also induced higher SOD1 expression ($P > 0.05$).

DISCUSSION

Liver toxicity is commonly observed in patients on long term antiretroviral therapy. No clear mechanism has been distinguished as individual ARVs have varying degrees of toxicity [Núñez, 2006]. Stavudine and AZT are considered among the most hepatotoxic NRTIs [Ter Hofstede et al., 2000; Wit et al., 2002] with TFV exhibiting very low hepatic toxicity [Birkus et al., 2002]. Hepatocytes possess cytoprotective mechanisms against xenobiotic insult. In this study, we assessed the mitochondrial and AO stress responses to NRTIs in liver cells after 24 and 120 h exposure.

The involvement of Nrf2 in the defence against NRTI-associated toxicity integrates two major mechanisms of NRTI toxicity– oxidative stress and mt toxicity. Firstly, Nrf2 regulates the transcription of AO genes during oxidative stress response [Motohashi and Yamamoto, 2004]. Secondly, the ARE to which Nrf2 binds in the nucleus shares motifs with transcription factor, NRF1 [Piantadosi et al., 2008]. This provides an overlap in the function of Nrf2 and PGC-1α, as both promote transcription of mtDNA via activation of NRF1. We observed that NRTIs increased Nrf2 and PGC-1α protein expressions, most so at 120 h (Fig. 3). Increased PGC-1α expression by NRTIs was also accompanied by lower ATP levels (Fig. 2A). Reduced ATP, an indication of reduced mt function, favours the activation of the AMP-activated protein kinase

pathway, which in turn increases mt biogenesis via PGC-1α and TFAM activity [Zong et al., 2002]. The upregulation of PGC-1α induced by NRTIs would not only promote mt biogenesis, but also increase the transcription of mt defence genes including manganese SOD and UCP2 [Valle et al., 2005] in response to mt oxidative stress.

Of the NRTIs evaluated in our study, TFV elicited the highest AO response, with a significant increase in the translational regulation of Nrf2 and its downstream target, SOD1 (Fig. 3). Tenofovir is considered one of the least toxic NRTIs and is commonly used in pre-exposure prophylaxis for HIV transmission prevention [Celum and Baeten, 2012]. At 120 h, TFV increased intracellular ROS (Fig. 1A) indicating early signs of mt oxidative stress. However, the strong antioxidant response in the TFV treated cells dampens oxidative damage so that lipid peroxidation is lower compared to AZT and d4T treated cells (Fig. 1B).

A previous study evaluating the cytotoxicity of TFV on HepG2 cells found that of five NRTIs tested, including AZT and d4T, TFV exhibited weak hepatic toxicity [Cihlar et al., 2002]. Furthermore, TFV is a weak inhibitor of DNA polymerase γ [Lewis et al., 2003], the enzyme responsible for mtDNA replication, and does not affect mtDNA content in HepG2 cells [de Baar et al., 2007]. Our study was consistent with this finding, as mtDNA levels were not depleted following 120 h exposure to TFV (Table I). However, we still found markers for mt dysfunction in TFV treated HepG2 cells (Fig. 2A and B). Studies assessing mt toxicity in TFV-induced nephropathy reported mt swelling and structural changes to mitochondria [Kohler et al., 2009; Abraham et al., 2013]. Our present study found that TFV caused a shift in mt membrane potential (Fig. 2B) which would compromise the integrity of the mt membrane. This can change the permeability of the mt membrane, promoting mt swelling. This mechanism of mt toxicity can occur independently of mtDNA depletion.

Thymidine analogues, AZT and d4T, are inhibitors of DNA polymerase γ [Bienstock and Copeland, 2004] and can therefore disrupt mtDNA replication. Various studies have investigated the effect of these two NRTIs on mt function and mtDNA in different cell lines with conflicting results. This suggests that AZT and d4T toxicity is tissue-specific and exposure time dependent. A study conducted by Banerjee et al. in 2013 reported AZT significantly increased oxidative stress markers in rat liver homogenates following acute exposure [Banerjee et al., 2013]. Another study comparing chronic exposure of endothelial cells to AZT and d4T found AZT increased oxidative stress and mt dysfunction, and not d4T [Kline et al., 2009]. However, work by Birkus et al. [2002] on HepG2 cells showed d4T was more toxic to mitochondria than AZT. Research by Velsor et al. [2004] on HepG2 cells corroborated that d4T exhibits mt toxicity and also induced mt oxidative stress. Our present work found AZT induced oxidative stress during early exposure (24 h) but markers for oxidative stress began to decline following 120 h exposure. Stavudine, however, only induced oxidative damage following 120 h exposure. The significantly lowered GSH levels in the d4T treated HepG2 cells (Fig. 1C) is likely to contribute to the elevated oxidative damage observed in this treatment. Both drugs exhibited mitochondrial toxicity (Fig. 2A and B), but this was more severe in the d4T treated cells. As d4T is the more potent inhibitor of DNA polymerase γ, and continually decreased mtDNA levels over time

(Table I), this may be a contributing factor to d4T being more toxic than AZT.

CONCLUSION

Our study found that NRTIs induced both the Nrf2 and PGC-1α stress responses, and this was highest in the TFV treatment. All drugs exhibited mt toxicity, especially at 120 h of exposure. Tenofovir induced mt dysfunction without reducing mtDNA levels. The d4T treatment showed the highest markers for oxidative stress at 120 h and lowest levels of mtDNA viability in HepG2 cells. We can conclude that Nrf2 and PGC-1α are very likely to play a role in the mt and oxidative stress response to NRTIs. Comparatively, d4T is the most likely NRTI to exhibit hepatotoxicity following prolonged exposure.

REFERENCES

Abraham P, et al. 2013. Depletion of the cellular antioxidant system contributes to tenofovir disoproxil fumarate - induced mitochondrial damage and increased oxido-nitrosative stress in the kidney. J Biomed Sci 20:1–15.

Banerjee A, et al. 2013. Zidovudine (AZT) and hepatic lipid accumulation: Implication of inflammation, oxidative and endoplasmic reticulum stress mediators. PLoS ONE 8:e76850.

Bienstock RJ, Copeland WC, 2004. Molecular insights into NRTI inhibition and mitochondrial toxicity revealed from a structural model of the human mitochondrial DNA polymerase. Mitochondrion 4:203–213.

Birkus G, et al. 2002. Assessment of mitochondrial toxicity in human cells treated with tenofovir: Comparison with other nucleoside reverse transcriptase inhibitors. Antimicrob Agents Chemother 46:716–723.

Bleeker-Rovers CP, et al. 2000. Hepatic steatosis and lactic acidosis caused by stavudine in an HIV-infected patient. Neth J Med 57:190–193.

Brinkman K, et al. 1998. Adverse effects of reverse transcriptase inhibitors: Mitochondrial toxicity as common pathway. AIDS 12:1735–1744.

Carr A, Cooper D A. 2000. Adverse effects of antiretroviral therapy. Lancet 356:1423–1430.

Celum C, Baeten J. 2012. Tenofovir-based pre-exposure prophylaxis for HIV prevention: Evidence and evolving questions. Curr Opin Infect Dis 25:51.

Chuturgoon AA, et al. 2014. Fumonisin B1 modulates expression of human cytochrome P450 1b1 in human hepatoma (Hepg2) cells by repressing Mir-27b. Toxicol Lett 227:50–55.

Cihlar T, et al. 2002. Tenofovir exhibits low cytotoxicity in various human cell types: Comparison with other nucleoside reverse transcriptase inhibitors. Antivir Res 54:37–45.

Cohen BH. 2010. Pharmacologic effects on mitochondrial function. Dev Disabil Res Rev 16:189–199.

Dagan T, et al. 2002. Mitochondrial dysfunction and antiretroviral nucleoside analog toxicities: What is the evidence. Mitochondrion 1:397–412.

de Baar MP, et al. 2007. Effects of apricitabine and other nucleoside reverse transcriptase inhibitors on replication of mitochondrial DNA in HepG2 cells. Antivir Res 76:68–74.

Igoudjil A, et al. 2007. High doses of stavudine induce fat wasting and mild liver damage without impairing mitochondrial respiration in mice. Antivir Ther 12:389.

Kline E, et al. 2009. Long-term exposure to AZT, but not d4T, increases endothelial cell oxidative stress and mitochondrial dysfunction. Cardiovasc Toxicol 9:1–12.

Kohler JJ, et al. 2009. Tenofovir renal toxicity targets mitochondria of renal proximal tubules. Lab Invest 89:513–519.

Lebrecht D, et al. 2009. Mitochondrial tubulopathy in tenofovir disoproxil fumarate-treated rats. J Acquir Immune Defic Syndr 51:258–263.

Lewis W, et al. 2001. Mitochondrial DNA depletion, oxidative stress, and mutation: Mechanisms 0f dysfunction from nucleoside reverse transcriptase inhibitors. Lab Invest 81:777.

Lewis W, et al. 2003. Mitochondrial toxicity of NRTI antiviral drugs: An integrated cellular perspective. Nat Rev Drug Discov 2:812–822.

Livak KJ, Schmittgen TD. 2001. Analysis of relative gene expression data using real-time quantitative PCR and the $2-\Delta\Delta CT$ method. Methods 25:402–408.

Mallon PWG, et al. 2005. In Vivo, nucleoside reverse-transcriptase inhibitors alter expression of both mitochondrial and lipid metabolism genes in the absence of depletion of mitochondrial DNA. J Infect Dis 191:1686–1696.

Manda KR, et al. 2011. Highly active antiretroviral therapy drug combination induces oxidative stress and mitochondrial dysfunction in immortalized human blood-brain barrier endothelial cells. Free Radic Biol Med 50:801–810.

Motohashi H, Yamamoto M. 2004. Nrf2-Keap1 defines a physiologically important stress response mechanism. Trends Mol Med 10:549–557.

Nedergaard J, et al. 2005. Uncoupling proteins: Current status and therapeutic prospects. EMBO Rep 6:917–921.

Núñez M. 2006. Hepatotoxicity of antiretrovirals: Incidence, mechanisms and management. J Hepatol 44:S132.

Phulukdaree A, et al. 2010. The effects of Sutherlandia frutescens extracts in cultured renal proximal and distal tubule epithelial cells. S Afr J Sci 106:54–58.

Piantadosi CA, et al. 2008. Heme oxygenase-1 regulates cardiac mitochondrial biogenesis via Nrf2-mediated transcriptional control of nuclear respiratory factor-1. Circ Res 103:1232–1240.

Roe AL, et al. 1993. HepG2 cells: An in vitro model for P450-dependent metabolism of acetaminophen. Biochem Biophys Res Commun 190:15–19.

Sambrook J, Russell D D W. 2001. Molecular cloning: A laboratory manual. New York: Cold Spring Harbour Laboratory Press.

Setzer B, et al. 2008. Pyrimidine nucleoside depletion sensitizes to the mitochondrial hepatotoxicity of the reverse transcriptase inhibitor stavudine. Am J Pathol 172:681–690.

St-Pierre J, et al. 2006. Suppression of reactive oxygen species and neurodegeneration by the PGC-1 transcriptional coactivators. Cell 127:397–408.

Stuart J, et al. 2004. DNA base excision repair activities and pathway function in mitochondrial and cellular lysates from cells lacking mitochondrial DNA. Nucleic Acids Res 32:2181–2192.

Ter Hofstede HJ, et al. 2000. Clinical features and risk factors of lactic acidosis following long-term antiretroviral therapy: 4 fatal cases. Int J STD AIDS 11:611–616.

Valle I, et al. 2005. PGC-1α regulates the mitochondrial antioxidant defense system in vascular endothelial cells. Cardiovasc Res 66:562–573.

Velsor LW, et al. 2004. Mitochondrial oxidative stress in human hepatoma cells exposed to stavudine. Toxicol Appl Pharmacol 199:10–19.

Venhoff N, et al. 2007. Mitochondrial toxicity of tenofovir, emtricitabine and abacavir alone and in combination with additional nucleoside reverse transcriptase inhibitors. Antivir Ther 12:1075.

Walker UA, et al. 2002. Increased long-term mitochondrial toxicity in combinations of nucleoside analogue reverse-transcriptase inhibitors. AIDS 16:2165–2173.

Wit FW, et al. 2002. Incidence of and risk factors for severe hepatotoxicity associated with antiretroviral combination therapy. J Infect Dis 186:23–31.

Zong H, et al. 2002. AMP kinase is required for mitochondrial biogenesis in skeletal muscle in response to chronic energy deprivation. Proc Natl Acad Sci 99:15983–15987.